Electronic Supplementary Information

Synthesis of visible light-active CeO_2 sheets via mussel-inspired $CaCO_3$ mineralization

By *Jong Wan Ko, Jae Hong Kim, and Chan Beum Park*
Department of Materials Science and Engineering, Korea Advanced Institute of Science and Technology (KAIST), 335 Science Road, Daejeon 305-701, Republic of Korea

Experimental Details

Materials: $CeCl_3.7H_2O$ (trace metal basis, 99.9%), dopamine-HCl, methylene blue (MB), NH_4OH (5.0 N), $CaCl_2$ (anhydrous and granular, 93%), CeO_2 (particle size <25 nm), Na_2CO_3, and other reagents were purchased from Sigma-Aldrich (St. Louis, USA) and used without further purification.

Synthesis of nano-grained CeO_2 sheets and CeO_2 flakes: PDA-induced $CaCO_3$ vaterite microspheres were synthesized according to our previous work with a slight modification. Briefly, we mixed 24 mL of $CaCl_2$ solution (0.33 M) with 24 mL of dopamine-HCl solution (2 mg mL^{-1}, 10 mM Tris buffer, pH 8.5) and 32 mL of NH_4OH solution (0.625 N). CO_2 gas was then introduced to the mixture at a flow rate of 0.3 L min^{-1} for 1 hour, and then the mixture was filtered and washed with deionized water. PDA-induced $CaCO_3$ vaterite was obtained from the filtered remnant dried under vacuum at room temperature. $CeCl_3.7H_2O$ was dissolved in deionized water (200 mL) to create a 0.1 M $CeCl_3$ solution. Under vigorous stirring, 1 g of PDA-induced $CaCO_3$ vaterite was slowly added to the $CeCl_3$ solution. The mixture was kept for 2 hours under stirring at ambient condition to produce $Ce_2(CO_3)_3.8H_2O$, which was collected, washed with deionized water, and dried at 323 K for 24 hours. Polycrystalline CeO_2 sheets were obtained by calcinating $Ce_2(CO_3)_3.8H_2O$ at different temperatures (573, 673, 813 K) under air atmosphere for 2 hours. For the synthesis of CeO_2 flakes, 0.1 M of $CeCl_3.7H_2O$ solution and 0.33 M of Na_2CO_3 solution were mixed at a 1:1 volume ratio under vigorous stirring. The precipitates were collected and dried for 24 hours at

323 K. By calcinating the precipitates at 813 K, CeO_2 flakes were obtained.

Photocatalytic reactions: Photocatalytic activities of CeO_2 sheets, and nanoparticles were measured by evaluating the degradation of MB under visible light irradiation. A reaction mixture was prepared by mixing 30 mg of CeO_2 sample in a 30 mL of MB solution (26.7 μM). Before light irradiation, the mixture was incubated in the dark for 2 hours under stirring to complete the equilibrium of adsorption-desorption of MB on the catalyst surface. The suspension was irradiated by a xenon lamp (450 W) with a 420 nm cut-off filter. To evaluate the degree of MB degradation, the absorbance of the photocatalytic reaction solution at 665 nm was measured after removing catalysts by centrifugation.

Characterization: The morphologies of each CeO_2 sample were observed using a S-4800 field emission scanning electron microscopy (Hitachi Co., Japan) at an electron acceleration voltage of 20 kV and Tecani F20 field emission transmission electron microscope (FEI Co., USA) with 200 kV of operating voltage. The X-ray diffraction patterns were recorded using a D/MAX-RB X-ray diffractometer (Rigaku Co., Japan) under a scan rate of 3 °/min, a scan range of 10 °- 70 °, and a Cu Kα radiation wavelength of 1.5418 Å. Absorbance spectra of CeO_2 sheets and nanoparticles were obtained using a UV-visible spectrophotometer (Jasco Inc., Japan) in a diffuse-reflectance mode. A Raman spectroscopic analysis was conducted using a high-resolution dispersive Raman microscope (Horiba Jobin Yvon, France). A spectrofluorometric study was performed using an RF-5301PC (Shimadzu Co., Japan) with an excitation wavelength of 265 nm. X-ray photoelectron spectroscopic analysis was carried out using a Sigma Probe (Thermo Scientific, UK) in the range of 0 – 1300 eV.

Elemental analysis: Elemental analysis was conducted using a Flash 2000 series (Thermo Scientific, UK). Followings are the result of the elemental analysis (wt%) for CeO_2 sheets calcinated at 573 K: N 0.00, C 0.52, H 0.34; calcinated at 673 K: N 0.00, C 0.83, H 0.20; calcinated at 813 K: N 0.00, C 0.13, H 0.13, and $Ce_2(CO_3)_3{\cdot}8H_2O$ sheets: N 0.00, C 6.73, H 2.21.

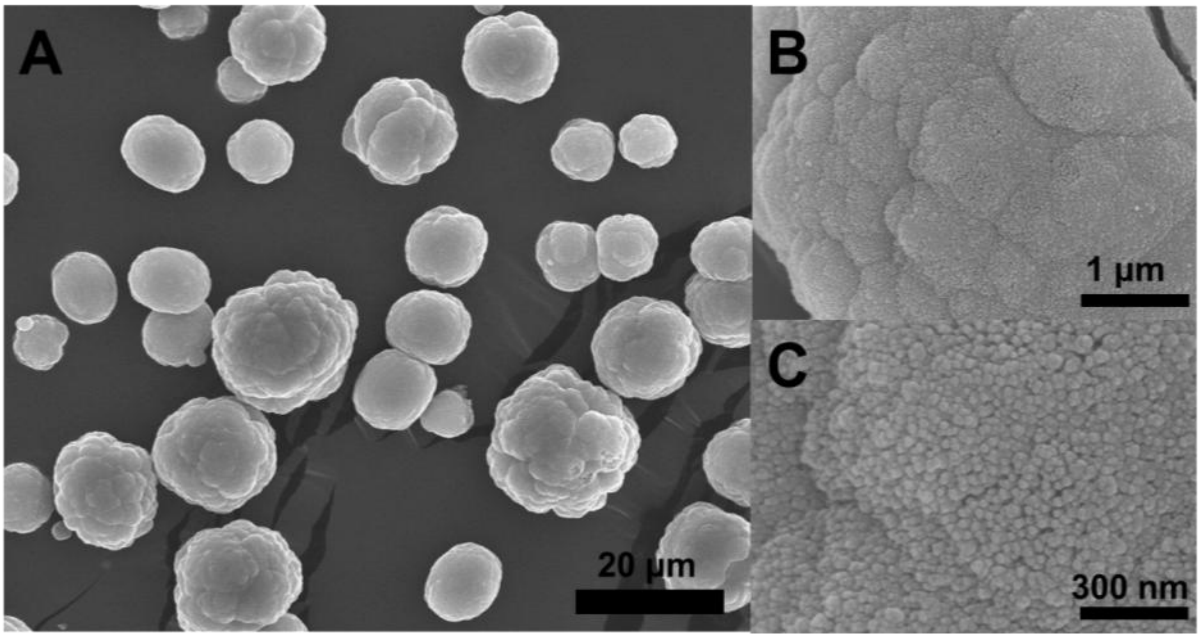

FIGURE S1. (A) SEM image of PDA-induced vaterite phase $CaCO_3$ microspheres. (B, C) Magnified SEM images showing that amorphous calcium carbonate (ACC) nanoparticles are well clustered to form spherical vaterite phase of $CaCO_3$ microstructure.

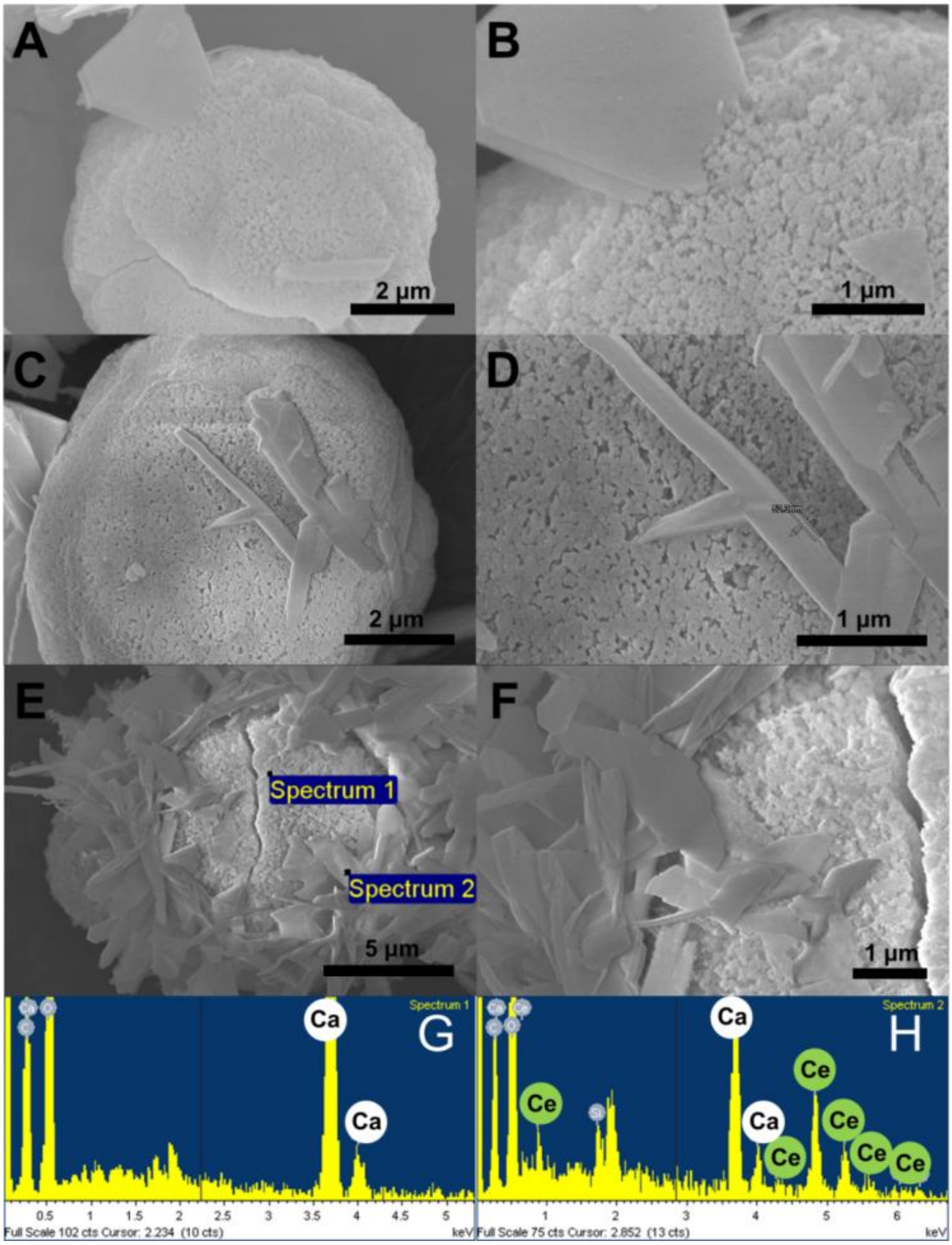

FIGURE S2. SEM images of PDA-induced $CaCO_3$ microspheres incubated in an $CeCl_3$ solution for 30 mins (A, B), 60 mins (C, D) and 90 mins (E, F). Energy-dispersive X-ray spectroscopic analysis of (G) deformed area of a vaterite microsphere and (H) newly formed sheet on the surface of the vaterite microsphere.

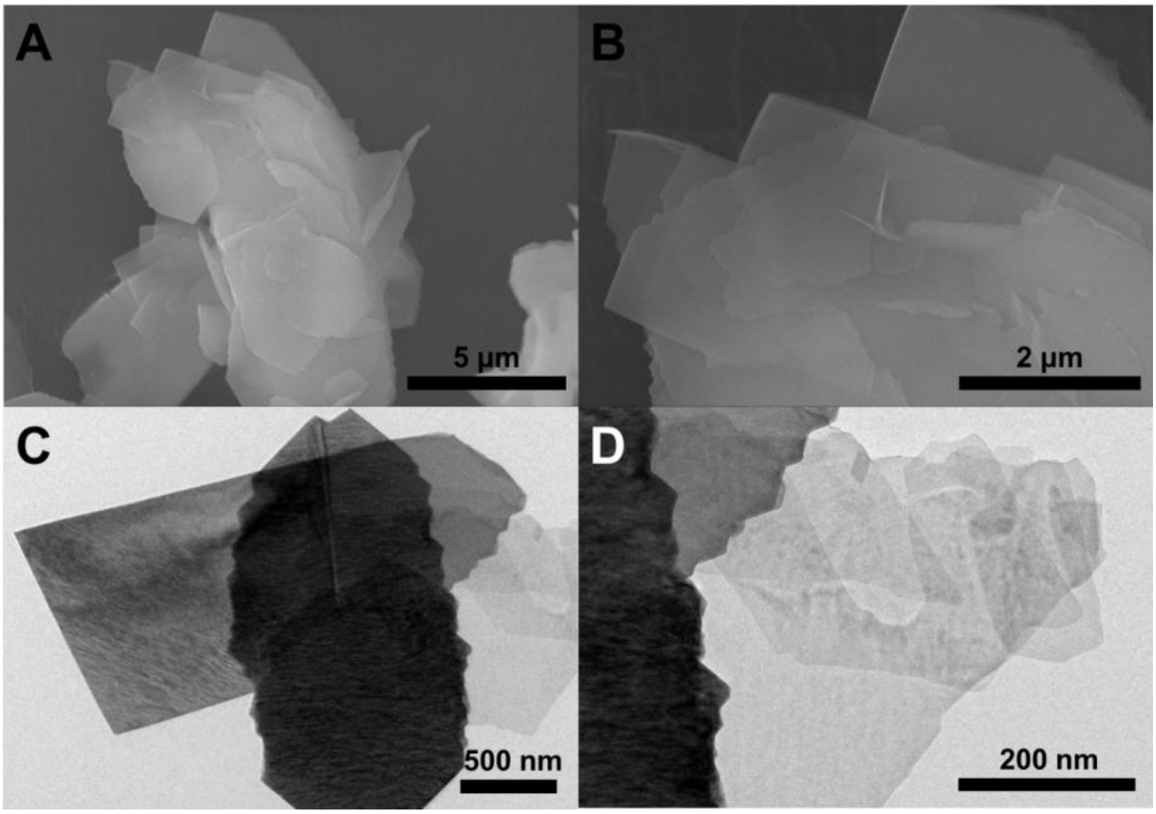

FIGURE S3. (A, B) SEM and (C, D) TEM images of sheet-like structure of $Ce_2(CO_3)_3 \cdot 8H_2O$ obtained with PDA-induced $CaCO_3$ vaterite microspheres after incubation under $CeCl_3$ solution for 2 hours are shown in different scales. Vaterite microspheres were completely dissolved and $Ce_2(CO_3)_3 \cdot 8H_2O$ sheets were formed.

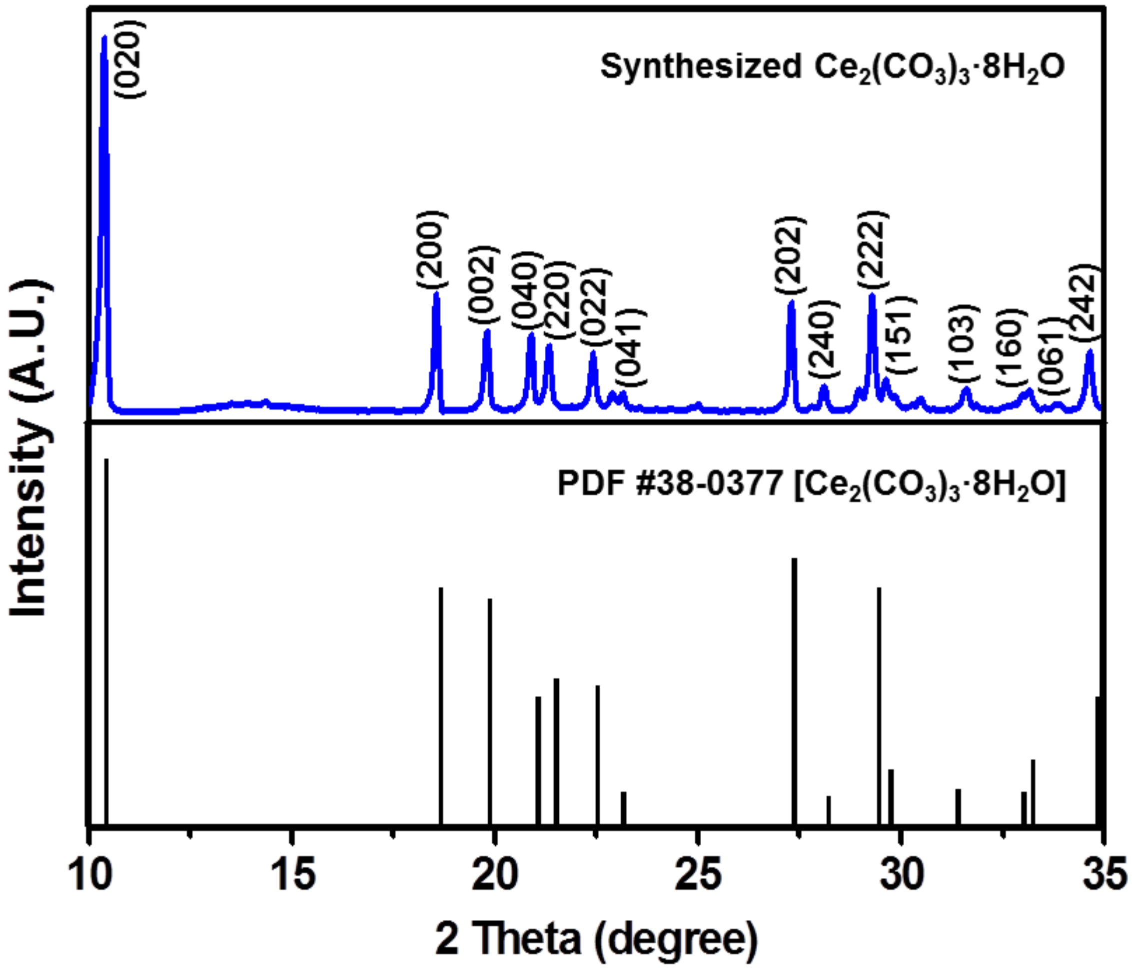

FIGURE S4. XRD pattern of sheet-like precipitates obtained from PDA-induced $CaCO_3$ vaterite microspheres incubated in $CeCl_3$ solution for 2 hours, which shows diffraction peaks corresponding to orthorhombic structure of $Ce_2(CO_3)_3 \cdot 8H_2O$ (JCPDS No. 38-0377).

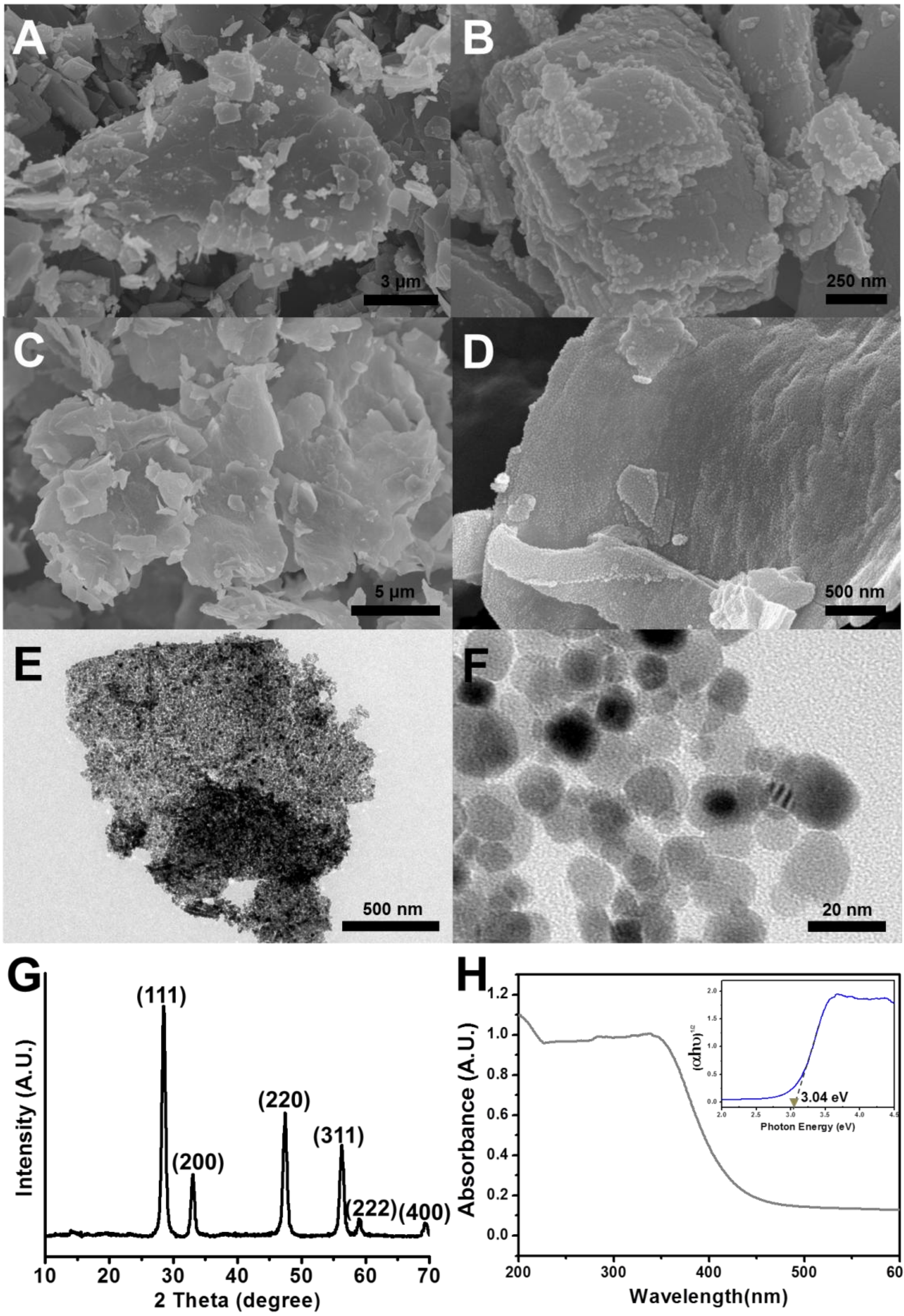

FIGURE S5. (A, B) SEM image of precipitates obtained after mixing $CeCl_3$ (0.1 M) and Na_2CO_3 (0.33 M) solution in 1:1 volume ratio. (C-F) SEM and TEM images of CeO_2 flakes attained from the precipitates after calcination at 813 K. (G) XRD pattern of CeO_2 flakes exhibiting typical diffraction peaks for CeO_2 (JCPDS NO. 34-0394). (H) UV-visible absorbance spectrum of the CeO_2 flakes. The inset figure shows the plot of the transformed Kubelba-Munk function versus light energy for CeO_2 flakes, indicating a bandgap of 3.04 eV.

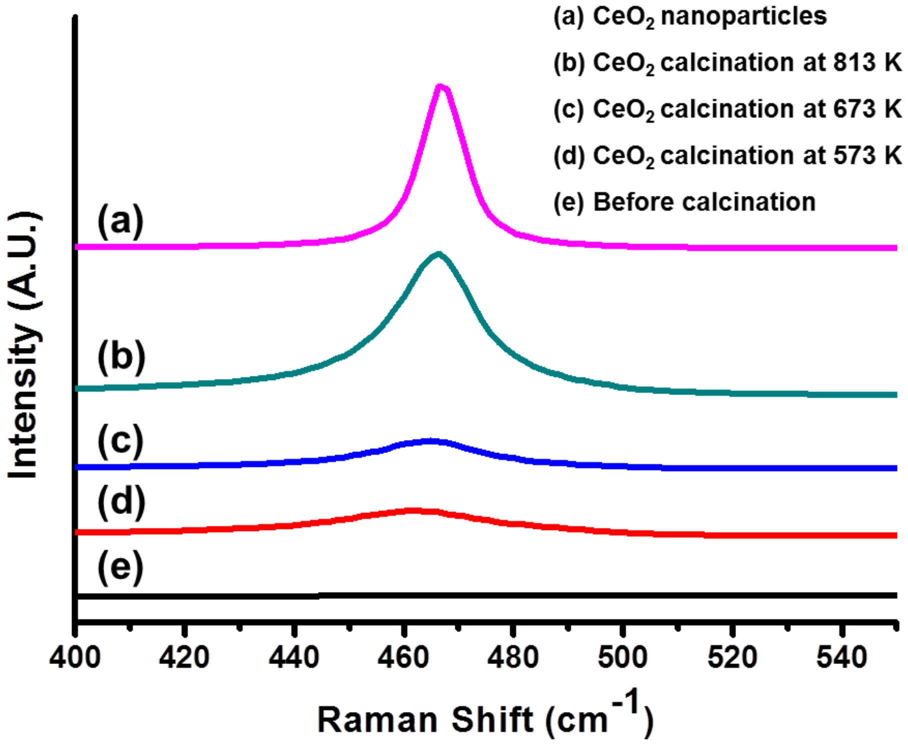

FIGURE S6. Raman spectra of (a) CeO_2 nanoparticles and nano-grained CeO_2 sheets calcinated at (b) 813, (c) 673, and (d) 573 K. The spectra show different degrees of Raman peak-broadening of a symmetric stretching mode of Ce-8O vibrational unit at around 466.28 cm^{-1}.

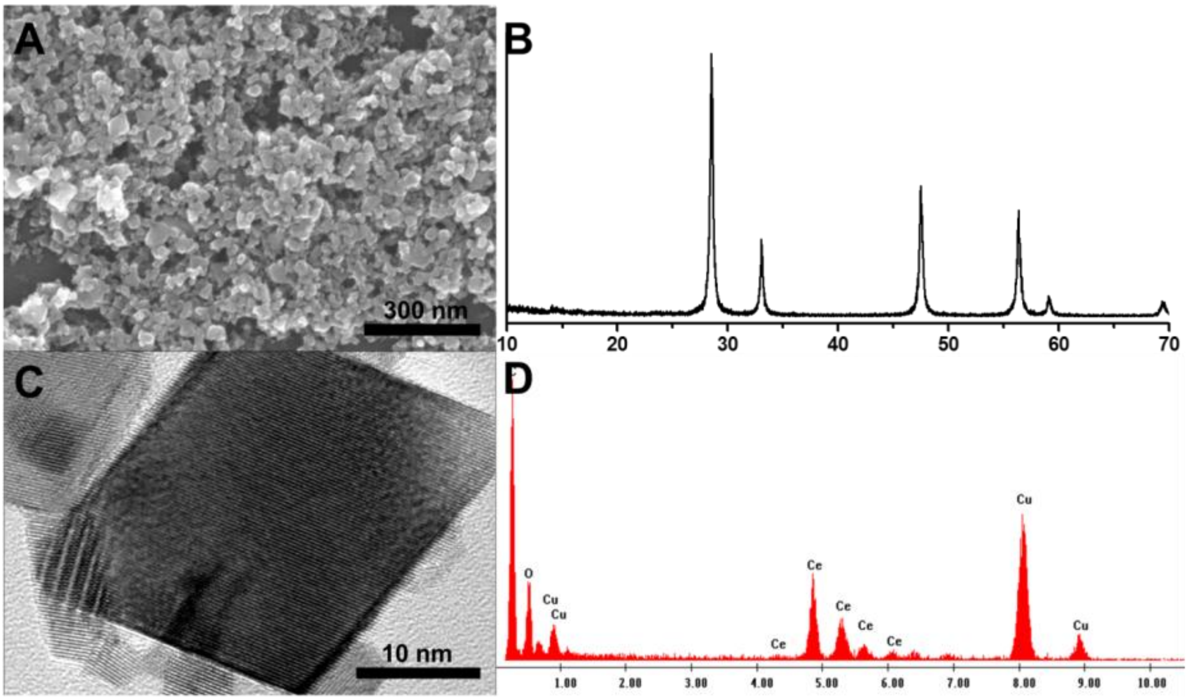

FIGURE S7. (A) SEM image and (B) XRD pattern of CeO_2 nanoparticles (purchased from Sigma-Aldrich Co., < 25 nm). (C) TEM image of the CeO_2 nanoparticles. (D) Energy dispersive X-ray spectroscopy spectrum of CeO_2 nanoparticles, which shows the existence of cerium and oxygen atoms. Note that copper atoms came from the TEM grid that was used for supporting the sample.

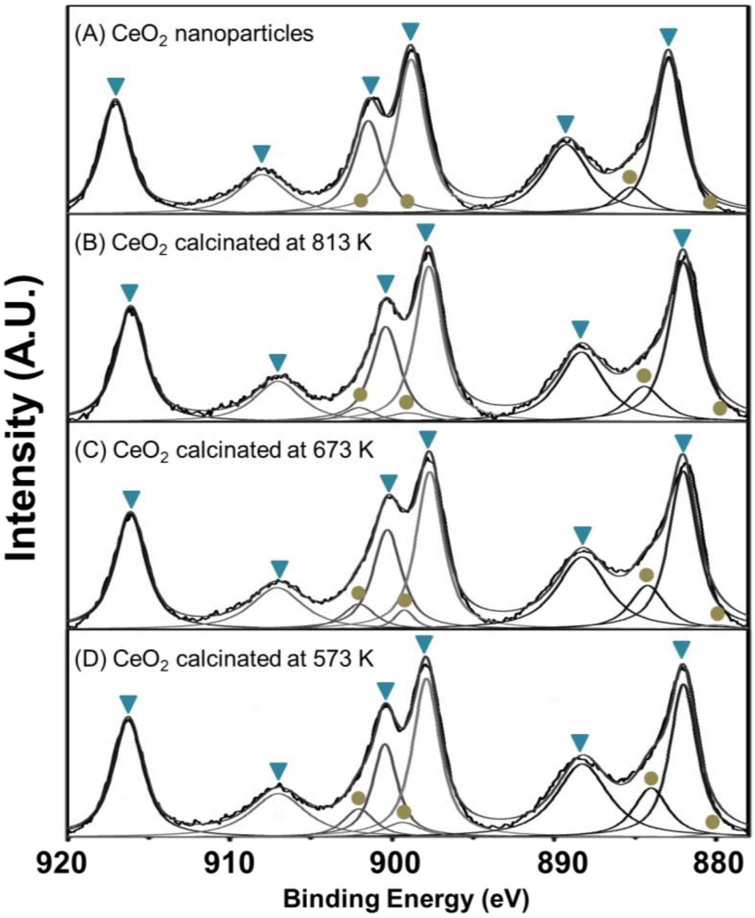

FIGURE S8. XPS spectra of nano-grained CeO_2 sheets and CeO_2 nanoparticles. The peaks between 895 and 910 eV originated from Ce $3d_{3/2}$, while peaks from 875 to 890 eV correspond to Ce $3d_{5/2}$. The peaks at 880.1 885.2, 899.2, and 902.0 eV are attributed to Ce^{3+} (circles) and the characteristic peaks of Ce^{4+} (triangles) are centered at 882.1, 888.1, 898.0, 900.8, 906.8, and 916.3 eV.

TABLE S1. The relationship among grain (or particle) size of CeO_2 samples, bandgap, and the ratio of cerium oxidation state in CeO_2 samples. The level of the oxidation state of cerium atoms was estimated from the integrated area of corresponding XPS peaks.

CeO_2 sample	**Estimated grain (or particle) size (nm) from Scherrer's equation**	**Bandgap (eV)**	**Ce^{3+}/Ce^{4+} ratio**
CeO_2 nanoparticles	23.5	3.13	0.13
CeO_2 calcinated at 813 K	13.3	2.83	0.17
CeO_2 calcinated at 673 K	8.2	2.74	0.20
CeO_2 calcinated at 573 K	6.2	2.71	0.23

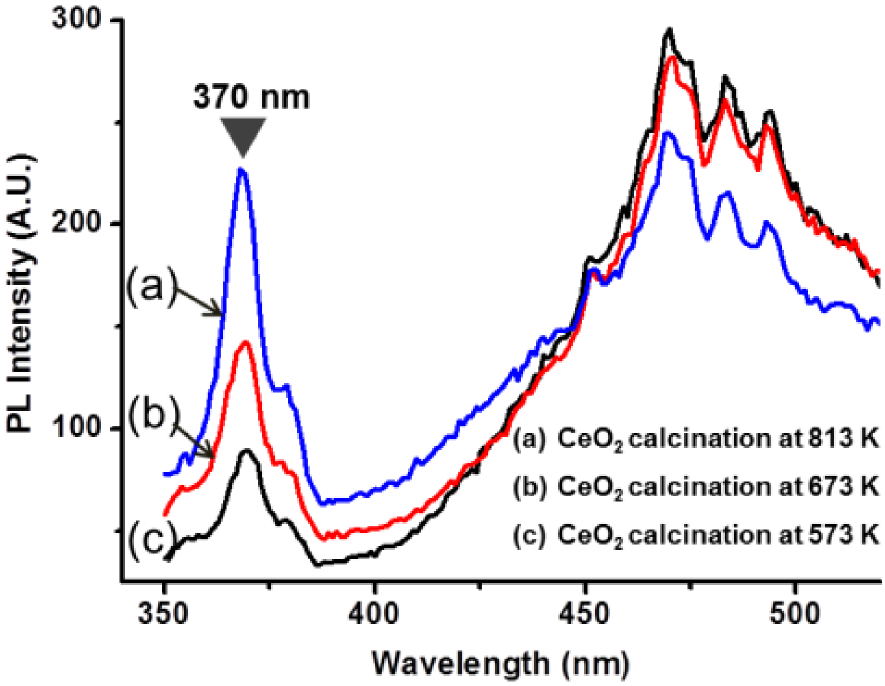

FIGURE S9. Room-temperature photoluminescence spectra of nano-grained CeO_2 calcinated at (a) 813, (b) 673, and (c) 573 K obtained with an excitation wavelength of 265 nm. The spectra show strong emission peaks at 370 nm and around 475 nm.

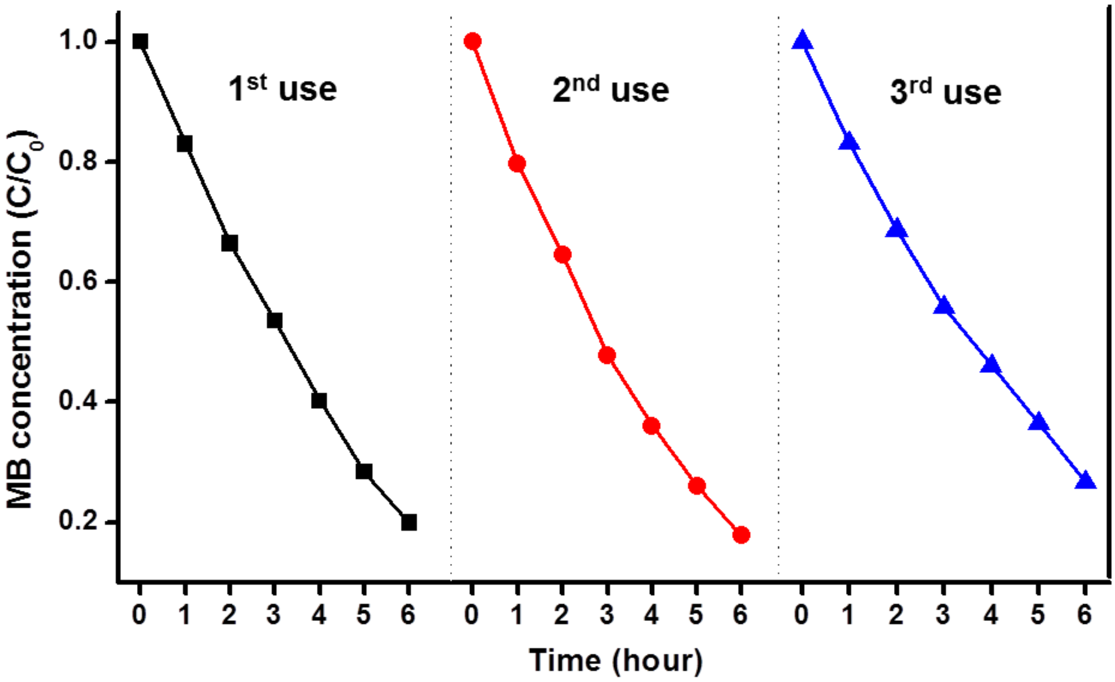

FIGURE S10. Photocatalytic activity of CeO_2 sheets calcinated at 573 K during repeated usage under visible light. The CeO_2 sheets were collected by filtration, rigorously washed with deionized water after each reaction, and dispersed in a MB solution (26.7 μM).